J. Min. Metall. Sect. B-Metall. 59 (2) (2023) 339 - 348

Journal of Mining and Metallurgy, Section B: Metallurgy

MICROSTRUCTURAL, MECHANICAL AND THERMODYNAMIC PROPERTIES INVESTIGATION OF THE NOVEL RARE EARTH-FREE MULTICOMPONENT Mg-15Al-8Ca-3Zn-2Ba ALLOY

Y. Türe

Eskisehir Technical University, Porsuk Vocational School, Electronics and Automation Department, Program of Mechatronics, Eskisehir, Turkey

(Received 08 March 2023; Accepted 02 November 2023)

Abstract

There has been a significant increase in research and development efforts to meet the growing demand for environmentally friendly magnesium (Mg) alloys. Studies are currently exploring different combinations of alloying elements to meet the demanding specifications. The aim of this study was to examine the usability of the elements aluminum (Al), calcium (Ca), and zinc (Zn) together with barium (Ba), and to investigate the mechanical and thermodynamic properties of the resulting multicomponent alloy system. SEM and hardness tests were used to examine the microstructural and mechanical properties of the Mg alloys. In the SEM analysis, the alloy was determined to consist of an α-Mg matrix, a block-like compact structure containing Ba ($Mg_{17}Ba_2$), a regional eutectic structure ($Ca_2Mg_6Zn_3$), and independently growing lamellae (Al_2Ca). The general hardness analysis results of the alloy, measured by Brinell and Vickers tests, were determined to be ~77 and ~82, respectively. The indentation test also revealed that the stress transfer to the Al_2Ca laves phase is possible, depending on the orientation of the slip plane between the matrix and the Al2Ca phase. It was also observed that cracks that developed on the intermetallic $Mg_{17}Ba_2$ phase in the indentation test were only formed in the high-stress regions of the structure, and their propagation was limited. According to the thermodynamic analysis, the ΔH_{mix} value is -2.73 kJ/mol, the ΔS_{mix} value is 5.95 J/molK, the δ value is 34%, the Δχ value is 0.14, and the Ω value is 2.03. The obtained thermodynamic data were found to be compatible with the microstructural development of the alloy.

Keywords*: Multicomponent Mg alloy; Light weight alloy; Low entrophy alloy (LEA); Microstructure*

1. Introduction

In today's world, where ecological and environmental problems are increasingly pressing, the potential benefits of technological advancements are being evaluated more than ever before. One area of research that has gained increasing attention is the development of lightweight materials. With this approach, studies on magnesium (Mg) and its alloys have become increasingly important due to their high specific strength properties. For example, as combating the climate crisis has become a top priority worldwide, the interest in light metal metallurgical technologies has grown due to their potential to reduce greenhouse gas emissions in transportation vehicles [1–3]. However, with the high production and raw material costs required to improve the mechanical, physical, and chemical properties of light materials such as Mg, there is a need to identify suitable elements to increase their plastic deformation capacity and corrosion resistance at ambient temperature. Numerous researchers continue to work on experimental and DFT-based ab initio approaches to enhance the properties of Mg using cheaper and more readily accessible alloying elements.

A review of the literature reveals that the studies on the alloying of Mg mostly involve combinations of elements such as Ca, Zn, Cu, Mn, etc. in addition to Al [4–10]. Besides, there is hardly any direct information about the impact of Ba on Mg apart from the phase diagram of the Mg-Ba binary alloy. However, research has been conducted on the impacts of the Ba element in ternary and quaternary Mg alloy systems. It has been reported that creep resistance at higher temperatures is significantly improved by a small amount of Ba (~ 0.02-0.03%) [11]. The bulky dimensions of the Ba-containing secondary phase contribute to the improvement of creep strength by effectively preventing grain boundary sliding [12]. According to J. Buha, the effects of the Ba element on Mg-Zn alloy were investigated. The addition of 0.2% Ba to the system significantly improved the age-hardening response of the Mg–2.8Zn alloy by stimulating the nucleation of precipitates and accelerating the kinetics of precipitation during aging. In fact, it was reported that the hardness of the Mg–

Corresponding author: yture@eskisehir.edu.tr

https://doi.org/10.2298/JMMB230308029T

2.8Zn–0.2Ba alloy increased approximately twofold due to the artificial aging process. J. Buha also stated in his study that the Ba element significantly increased the solidification temperature, thus providing a wider temperature range for mechanical processing [13].

Conventionally defined alloys (we can consider them as LEA) are systems rich in one major element but poor in other alloying elements. Studies on multicomponent alloy systems of Mg (MCA-Mg) continue to increase due to their potential to offer better properties than conventional Mg alloys.

There are studies in the literatura with different elements and different amounts of alloying elements in the MCA-Mg type (e.g. MgAlCuMnZn, MgAlZnCuCe, MgAlZnSnBi, etc.) [14–16]. By increasing the number and amount of alloying elements, a more entropically disordered structure can be obtained. Thus, it will be possible to create an alloy system consisting of a soft, Mg-derived matrix phase and secondary phases with higher strength within this structure. In this approach, the required excellent strength and ductility can be obtained together, and the application range for magnesium can be extended. Moreover, different studies evaluating the modulus of elasticity have reported that MCA-Mg alloys have ~20-25% higher modulus of elasticity compared to pure Mg [17–19]. Especially in multi-phase systems, it is very important to determine the deformation permeability of the phases in addition to the specific behavior of each phase. M. Zubair et al. presented a study that used micro indentation and nanoindentation techniques, to show the co-deformation mechanism between the hard Laves phases and the soft Mg matrix phase occurring in the Mg-Al-Ca alloy.

According to this study, the deformation zone both above and below indents in the a-Mg matrix was found to be influenced by the orientation and the neighboring Laves phases. The sub-surface deformation mechanisms are effectively represented by the deformation around surface indents. Remarkably, the Laves phase and the α-Mg matrix undergo co-deformation, even though the Laves phase is considerably harder than the α-Mg phase. Evidence of this is the observation of slip lines in the Laves phase, particularly in regions where they intersect with slip lines or twins in the α-Mg matrix. The deformation of the α-Mg phase involves various mechanisms such as mechanical twinning, basal and non-basal slip. In this study by Mzubair et al., it was notably observed that the dominant mechanism was basal slip [20].

The objective of this study is to determine the microstructural, mechanical, and thermodynamic properties of a multicomponent Mg alloy (Mg-15Al-8Ca-3Zn-2Ba). Additionally, the study aims to investigate the possible deformation permeability between phases and examine the effects of elements commonly used in Mg alloys, such as Al, Ca, and Zn, as well as the influence of adding Ba to the alloy system. This inclusion adds a separate dimension to the research.

2. Experimental Details

The alloy used in the study was obtained by melting the components of Al, Zn, Ca and Ba in an argon (Ar) atmosphere in a steel crucible in quantities determined by mass. An atmosphere-controlled chamber furnace (MSE Furnace-Turkey) was used for the production of the alloy. The melting process was conducted at 750 °C for 10 minutes. Afterward, the furnace was turned off and the sample was allowed to cool in the Ar atmosphere. After the melting process, no additional heat treatment was applied to the alloy. The alloy was then precision cut to a size of 2 cm x 2 cm and cold molded. The molded sample was subjected to appropriate grinding (500, 800, 1000, and 2000 grade SiC papers) and polishing (3µm and 1µm diamond solutions) processes, respectively. Finally, the sample was prepared for analysis by etching with a picric acid-based solution.

The microstructural examination was performed using a scanning electron microscope (SEM - ZEISS SUPRA 50 VP) equipped with an X-ray energy spectrometer (EDS - Oxford Instruments) analyzer. The phase composition of the alloy was determined using X-ray diffraction (XRD) analysis, using a a MiniFlex 600 instrument. The analysis was conducted in the 2θ range of 20–75°, at a scanning speed of 0.5°/min, using Cu-Kα radiation. The hardness measurements of the alloy and the indent required to determine of the deformation properties were carried out using the hardness device (EMCO Test - M1C010).

Thermodynamic parameters such as mixing enthalpy (ΔH_{mix}), mixing entropy (ΔS_{mix}), atomic size difference (δ), electronegativity (Δχ), and Ω were calculated for the alloy with nominal composition Mg-15Al-8Ca-3Zn-2Ba using appropriate Equations (1) – (5) and values [21–23]. The mixing enthalpy (ΔH_{mix}) of the solid solution had determined by the following equation according to the regular solution model:

$$\Delta H_{mix} = \sum_{i=1, i\neq j}^{n} 4\Delta H_{AB}^{mix} C_i C_j \quad (1)$$

where ΔH_{AB}^{mix} is the enthalpy of mixing of constituent binary alloys, C_i and C_j is the atomic percentage of the ith and jth component.

The configurational entropy of mixing (ΔS_{mix}) during the formation of regular solution alloy had calculated by:

$$\Delta S_{mix} = -R\sum_{i=1}^{n} C_i \ln\left(C_i\right) \quad (2)$$

Here R is the universal gas constant. The δ parameter is a parameter that examines the relationship between phase stability and percent atomic size difference and was calculated with the following equation:

$$\delta = 100x[\sum_{i=1}^{n} C_i(1-r_i/r_a)^2]^{1/2} \quad (3)$$

where r_i is the radius of a given element and r_a is the average atomic radius $(r_a = \sum_{i=1}^{n} r_i C_i)$.

The electronegativity difference in a multicomponent alloy system was determined by the equation:

$$\Delta\chi = [\sum_{i=1}^{n} C_i(\chi_i - \chi_a)^2]^{1/2} \quad (4)$$

where $\chi_a = \sum_{i=1}^{n} C_i\chi_i$ and χ_i refers to the Pauling electronegativity for the i*th* component. The Ω parameter has been proposed as a means to predict the solid solution-forming ability of multicomponent alloy systems. The following equation was used to determine this parameter:

$$\Omega = \frac{T_m \Delta S_{mix}}{\left|\Delta H_{mix}\right|} \quad (5)$$

where T_m $(T_m = \sum_{i=1}^{n} C_i(T_m)_i)$is the melting point of the alloy ($(T_m)_i$ is the melting point of the ith component).

3. Results and Discussion

3.1. Microstrucutral features

The microstructural features of the alloy were examined using the SEM-BSE detector, and a general view of the microstructure is presented in Fig. 1. The alloy is composed of an α-Mg matrix, a block-like compact structure containing Ba (white-colored phase), a regional eutectic structure (light gray-colored phase), and independently growing lamellae (dark gray-colored phase) spread over a large area. The phase analysis, carried out using ImageJ, reveals that the α-Mg (matrix phase) accounts for about 80% of the entire structure, while the ratios of the light gray-colored lamellae and widely spread dark gray-colored lamellar regions are determined to be ~ 8% and ~ 7%, respectively. Additionally, the white phase in the block structure rich in Ba element accounts for ~ 5% of the entire structure. The block-like structure of Mg-Ba-based intermetallic is consistent with the limited literature sources [24,25].

The chemical compositions of the constituent phases in the alloy were determined using the SEM-EDS detector. EDS point analyses were conducted at specific locations to provide detailed information on the elemental distribution within the microstructure. The areas selected for point analyses are illustrated in Fig. 1 and the EDS results are presented in Table 1. Notably, despite the high aluminum content in the Mg alloy system, no evidence of $Mg_{17}Al_{12}$ phase formation was observed via EDS analysis. This finding may be attributed to the high calcium content previously reported in the literature [26,27].

The white phase, characterized by its high atomic weight and rich in Ba, corresponds to the blue point in

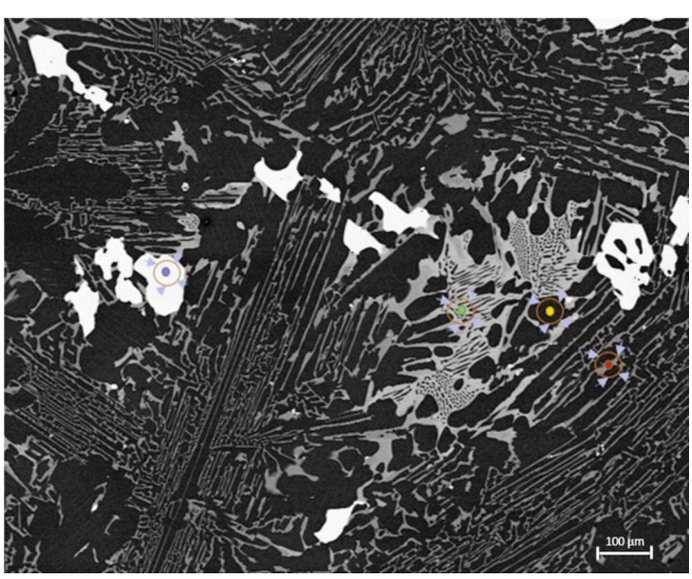

Figure 1. *General microstructure image of the alloy and colored dots showing different regions where EDS spot analyzes were performed*

Table 1. *EDS analysis of the different microstructural constituents and corresponding possible phases [23,26]*

Point color	Element	at. %	Possible Compound
Yellow	Mg	100	α-Mg
Blue	Mg	81.16	$Mg_{17}Ba_2$
	Ba	8.15	
	Al	6.28	
	Zn	3.58	
	Ca	0.81	
Red	Mg	7.17	Al_2Ca
	Al	61.22	
	Ca	31.61	
Green	Mg	59.07	$Ca_2Mg_6Zn_3$
	Al	12.65	
	Ca	14.67	
	Zn	13.61	

the microstructure and was mostly observed to develop on dark-colored eutectic components. Previous studies suggest that this phase corresponds to $Mg_{17}Ba_2$ phase [25]. The result of EDS analyses performed with 20 kV indicates that the element Al comes from the eutectic component on which it occurs as an effect of electron-sample interaction. The dark gray eutectic component, identified as the red dot in the EDS point analysis, was found to contain 61.22% Al and 31.61% Ca, indicating the presence of the Al_2Ca phase [28,29]. The light gray phase, represented by the green color, is consistent with the $Ca_2Mg_6Zn_3$ phase observed in previous studies [30,31]. This phase displays partially divorced eutectic characteristics when examined microstructurally. The result of the XRD analysis of the sample is presented in Fig. 2. The intermetallic components of Al_2Ca (XRD reference code: 01-075-0875), $Mg_{17}Ba_2$ (XRD reference code: 00-018-0173), and $Ca_2Mg_6Zn_3$ (XRD reference code: 00-012-0266) in the structure are shown by markings on the graph. These results are consistent with the EDS analysis.

The microstructure of the alloy has also been evaluated in terms of stacking fault energy (SFE) within the study. Each alloying element utilized in the research was found to decrease the SFE of Mg, as demonstrated by previous ab initio calculations in the literature [32]. When considering the SFE concept in a general evaluation of the microstructure, it is expected that the lamellar structure will be the dominant secondary phase in the alloy due to the decreasing nucleation and growth energy of the lamellar phases with decreasing SFE values [33].

3.2. Thermodinamical approach

The thermodynamic properties of a MgAlCaZnBa alloy, composed of five distinct non-equimolar components, were investigated using equations commonly employed in multicomponent alloy systems, particularly in the design of high entropy alloys (HEAs). However, since the present alloy does not exhibit an equimolar or near-equimolar distribution of elements, it is inappropriate to classify it as a HEA, which has been a topic of considerable research interest lately. This conclusion was confirmed by thermodynamic calculations, and the details of the calculations, including the formulas and

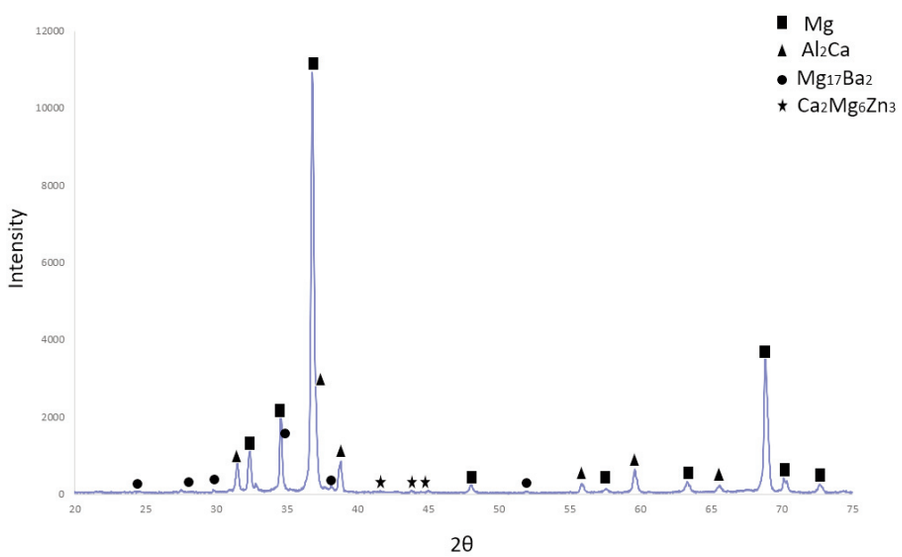

Figure 2. *XRD patterns of MCA-Mg alloy*

values used, are provided in the experimental section. The computational results are presented in Table 2.

The thermodynamic parameter ΔH_{mix} is essential for assessing the chemical compatibility between key components in alloys [16,21,34–39]. A negative ΔH_{mix} value indicates a higher probability of intermetallic compound formation in the alloy. In our study, the calculated ΔH_{mix} value for the alloy was -2.73 kJ/mol, which is consistent with the presence of intermetallics. Conversely, a positive ΔH_{mix} value would result in a reduced mixing of the alloy components in the liquid state, potentially leading to the formation of segregations in the final alloy. Furthermore, previous literature indicates that a ΔH_{mix} value approaching zero may lead to the formation of a stable solid solution phase due to the random dispersion of elements in the alloy [39,40].

Table 2. *Calculation results of various thermodynamic parameters for Mg-15Al-8Ca-3Zn-2Ba multicomponent alloy*

ΔH_{mix} (kJ/mol)	ΔS_{mix} (J/molK)	δ (%)	Δχ	Ω
-2,73	5,95	34	0,14	2,03

The alloy investigated in this study should be considered a typical multicomponent alloy due to the diverse range of components it contains. Therefore, the ΔS_{mix} value cannot be expected to be as high as in alloys with high-entropy alloy (HEA) properties, which contain almost equal proportions of alloying elements. The measured value of 5.95 J/molK is much lower than the range of 11-19 J/molK predicted in the literature. Additionally, the atomic misfit (δ) value, an important parameter for HEAs, must satisfy the δ<6% criterion. However, the δ value calculated for the investigated alloy was 34%, indicating a higher tendency for intermetallic compound formation within the structure [40–43]. The values of Δχ and Ω, which were calculated in this study and are commonly used to evaluate solid solution formation in HEA systems, were found to be 0.14 and 2.03, respectively. Previous studies have reported solid solution formation in the system when Δχ is less than 0.175 and Ω is greater than 1 [16,34,38,40]. Our calculated values allow a discussion on the formation of solid solutions in our alloy system.

3.3. Microhardness test and deformation response of the alloy

The mechanical properties of the investigated alloy were evaluated using Vickers (HV) and Brinell (HB) hardness tests, and the results are presented in Table 3. Consistent with prior expectations, both the HV and HB values exhibited a significant increase relative to pure Mg. Specifically, the alloy demonstrated a 207% increase in HV value and a 156% increase in HB value compared to pure Mg. These enhancements can be attributed to the secondary phases present in the alloy structure, notably the $Ca_2Mg_6Zn_3$ phase and Al_2Ca laves phase, which are the primary constituents of the structure after the α-Mg. Although the intermetallic $Mg_{17}Ba_2$ also contributes to the mechanical properties, analysis of the relevant binary phase diagrams suggests that the contribution of this intermetallic to strength may be relatively less significant due to the higher melting point of Al_2Ca.

Table 3. *Vickers (HV) and Brinell (HB) microhardness test results of the alloy*

Alloy	HV1/10	HB1/5/10
Mg-15Al-8Ca-3Zn-2Ba	81.96 ± 2.5	76.86 ± 1.9

The purpose of the hardness tests is to examine the behavior of the intermetallic Al_2Ca, which is one of the important laves phases dominating the microstructure, and the intermetallic $Mg_{17}Ba_2$ formed by Ba, which is a limited research resource in the literature, under applied force. To investigate the deformation response of the heterogeneous microstructure of the alloy under external forces, the effect of the hardness test on the microstructure was visually examined using the SEM-BSE detector. The results showed crack formations in the intermetallic phases near the indentation. However, no separation between the second phase and the matrix was observed.

The microstructure of Mg-Al-Ca alloy systems in previous studies indicates that the Laves phase typically forms a network structure [29,44–46]. In the alloy microstructure that we examined within the scope of this study (as shown in Fig. 1), we observed that the Al_2Ca Laves phase was elongated in certain directions, with fewer connections between them compared to the networked structure. This component of branched plates has fewer interactions with each other, which means that the amount of stress absorbed by the soft α-Mg in the alloy is greater. Thus, the process results in limited crack formation as shown in Figure 3(a). This is in contrast to an alloy system with a fully interconnected skeleton structure, as shown in Fig. 3(b) [29], where larger cracks are observed. However, the other continuous eutectic morphology in Fig. 3(c) exhibits the same stress transmission pattern as Fig. 3(b).

In accordance with prior research, in addition to the formation of cracks in the Laves phases in close proximity to the indentation, parallel slip lines were also observed on the sample surface surrounding the indentation, as depicted by the blue arrow in Fig. 4. The overlapping locations of these slip lines at the interface between the α-Mg matrix and the Al_2Ca

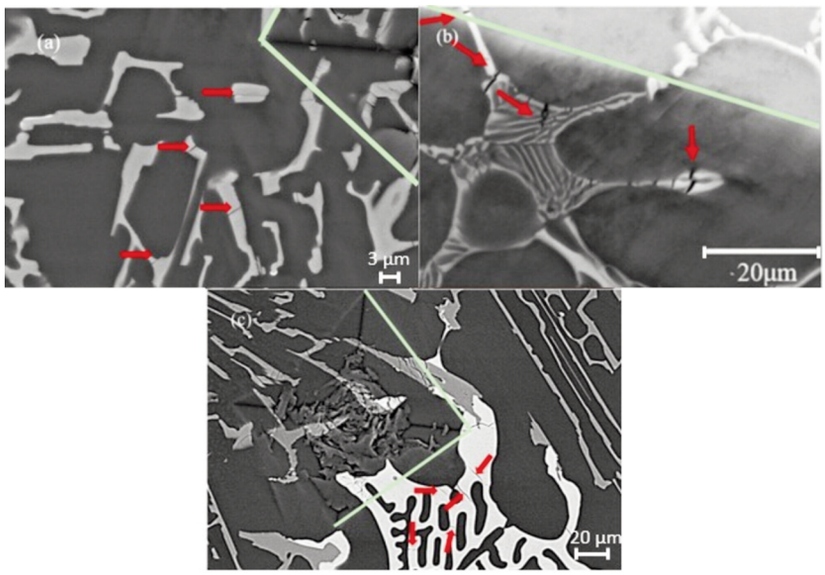

Figure 3. *SEM-BSE images taken near the indent in the Vickers microhardness test (a,c) Mg-15Al-8Ca-3Zn-2Ba, (b) Mg-4Al-4Ca [28] (Red arrows show cracks and green lines show indent boundary)*

Laves phase suggest that deformation and cracks occur simultaneously in both phases. This phenomenon is supported by the high probability of crack formation due to slip interaction, as observed in the study by M. Zubair et al. (Fig. 5) [47].

When analyzing the results from the perspective

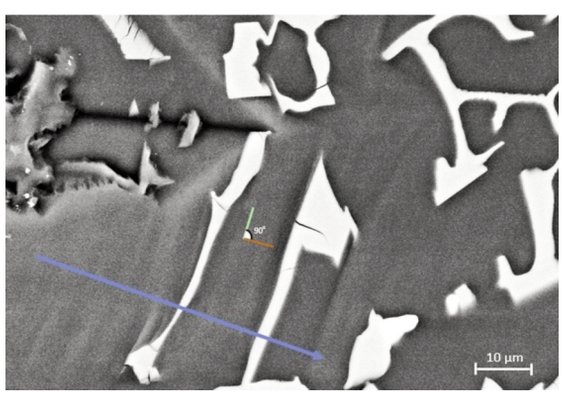

Figure 4. *SEM-BSE image showing the relationship between cracks and slip plane*

of critical resolved shear stress (CRSS), the observed behavior contradicts expectations. The CRSS value of the Al_2Ca Laves phase is approximately seven times greater than that of α-Mg, making the occurrence of this transfer a formidable task [48]. Furthermore, this situation coincides with the fact that the hardness at the α-Mg-Laves phase interfaces in the literature is higher than the hardness observed for the α-Mg phase [20]. However, evidence supporting this stress transfer phenomenon can be found in Fig. 4, where cracks on the Laves phase are clearly visible. This situation is typically attributed to two primary factors. Firstly, in Mg alloys, alloying elements, precipitates, grain, and phase boundaries affect the activation energy necessary for non-basal slip plane deformation, leading to inevitable differences between experiments conducted on single crystals and polycrystalline structures. Secondly, when two structures with different hardness values are present (here, Al_2Ca >> α-Mg), dislocation slip occurs in the soft phase, and dislocation pile-up occurs at the phase boundary due to obstruction from the hard phase. This phenomenon leads to a gradual increase in the stress concentration between the two phases, prompting the system to trigger dislocation movement in the hard phase to balance this increase [20]. Examination of Fig. 4 reveals that the slip planes indicated by the blue arrow in the Mg matrix phase cause cracks in the Al_2Ca phase. Additionally, the fact that the angle between the slip planes and cracks is geometrically 90 degrees serves as strong evidence of stress transfer.

Fig. 6 depicts the area where the indentation process was performed on the $Mg_{17}Ba_2$ phase containing the Ba element. It is evident that the cracks that developed on the intermetallic structure did not propagate from one end of the phase to the other. This phenomenon is more distinct, especially in the region where the green lines indicating the direction of the cracks are located. Another noteworthy observation is the difference in crack propagation between the regions outside the indent trace, as indicated by the green and orange lines. While the cracks in the lower part of the indent are oriented perpendicularly to the trace, the cracks on the upper face of the indent progressed parallel to the trace. Due to the scarcity of studies on Mg-Ba alloys in the literature, a definite evaluation of CRSS could not be conducted.

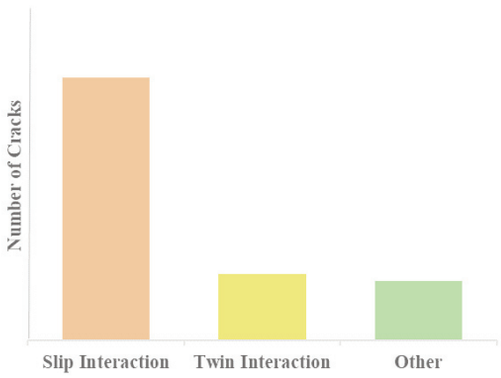

Figure 5. *The proportion of cracks appearing at α-Mg/Laves phase interfaces, slip plane intersection, and twin intersection. (Here, "others" refers to different cracks that do not originate from the slip plane interface or the twin interface intersection) [44]*

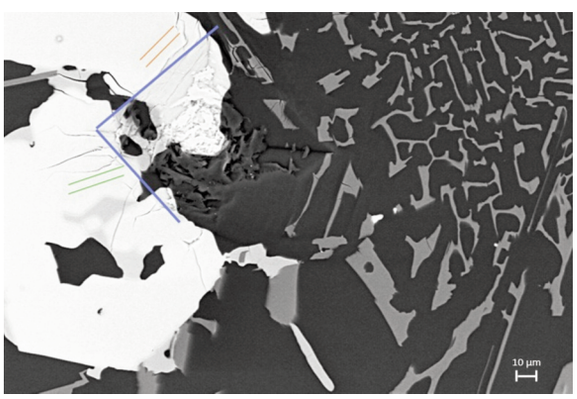

Figure 6. *SEM-BSE image of the indent on the $Mg_{17}Ba_2$ intermetallic*

3.4. Evaluation based on SRO

Based on Miedema's model for binary Mg alloys, Abaspour and Caceres evaluated the potential formation of short-range order (SRO) in the alloying elements used. This suggests that the α-Mg regions in the microstructure may contain limited solid solution structures with SRO [49]. It is possible that these structures cannot be identified through EDS analysis due to their low solubility and limited A-B-A order (where A represents Mg and B represents an alloying element). However, future nanoindentation tests on the α-Mg region could reveal the SRO structure formed by the alloying elements and provide nanohardness values higher than pure Mg (~0.9 GPa) [50].

4. Conclusion

Within the scope of the study, Mg-15Al-8Ca-3Zn-2Ba alloy was investigated in terms of microstructure, deformation behavior and thermodynamics. The results of the study are summarized as follows:

- The microstructural characterization of the multicomponent Mg-15Al-8Ca-3Zn-2Ba alloy was performed using SEM-EDS and revealed the presence of four different components. These are the α-Mg matrix, the $Mg_{17}Ba_2$ phase with a block-like compact Ba, the $Ca_2Mg_6Zn_3$ phase with a regional eutectic structure, and the widely distributed independently developing lamellar Al_2Ca phase. These results were found to be consistent with the phase analysis using XRD.
- The calculated negative ΔH_{mix} value is an important indicator of the presence of intermetallics in the alloy structure and is consistent with the microstructural diversity of the alloy used in the study. The ΔS_{mix} value was calculated to be 5.95 J/molK, which is not as high as in systems containing almost equal proportions of alloying elements. In addition, the atomic mismatch (δ) value, an important parameter for multi-element systems, was calculated to be 34%, indicating a significant tendency to form intermetallics. The $\Delta\chi$ and Ω values calculated in this study, frequently used to determine the solid solution formation potential of the alloy systems, were found to be 0.14 and 2.03, respectively. The $\Delta\chi$ value indicates the presence of a solid solution in our alloy system, making possible SRO analyses appropriate.
- The microhardness of the developed MCA-Mg alloy was determined as HV 81.96 and HB 76.86, respectively. The alloy exhibited a significant increase in microhardness, attributed to the contribution of secondary phases in the alloy structure. This increase is further supported by microstructure and thermodynamic data, indicating a higher level of hardness compared to most conventional Mg-based alloys.
- Examination of the impact area of the hardness test indentation revealed a 90-degree relationship between the slip lines and cracks at the interface between the α-Mg matrix and the Al_2Ca phase, indicating deformation permeability between the phases.
- Upon examination of the indent trace resulting from the hardness test on the $Mg_{17}Ba_2$ intermetallic and its surroundings, it became apparent that the intermetallic structure experienced less deformation compared to α-Mg. Additionally, the formed cracks were not confined to one direction but rather could be oriented both parallel and perpendicular to the indent.

Acknowledgements

The author is immensely thankful to the Eskisehir Technical University (ESTU) – Materials Science and Engineering Department, "Electron Microscopy Team" for SEM analysis support. Further, the author

states that he is grateful for the valuable help of Prof. Dr. Ali Arslan Kaya.

Authors Contributions

Y. Türe: Conceptualization; Data curation; Formal analysis; Investigation; Methodology; Validation; Visualization; Writing-original draft.

Data availability

Data available on request from the authors.

Conflict of Interest Statement

The authors have no conflicts of interest to declare.

References

[1] Y. Türe, C. Türe, Environmental and economic effects of fuel savings in driving phase resulting from substitution of light metals in european passenger car production, Transportation Research Record, 2675(9) (2021) 1163–1174. https://doi.org/10.1177/03611981211006418

[2] Y. Türe, C. Türe, An assessment of using aluminum and magnesium on CO2 emission in European passenger cars, Journal of Cleaner Production, 247 (2020) 119-120. https://doi.org/10.1016/j.jclepro.2019.119120

[3] M. Vončina, M. Petrič, P. Mrvar, J. Medved, Thermodynamic characterization of solidification and defects that occur in Mg-alloy AM60, Journal of Mining and Metallurgy, Section B: Metallurgy 53(2) 2017 107–14. https://doi.org/10.2298/JMMB160609009V

[4] Z.M. Hua, M.X. Li, C. Wang, X. Shi, Z.Y. Meng, Y.J. Li, H.L. Jia, M. Zha, H.Y. Wang, Pre-strain mediated fast natural aging in a dilute Mg-Zn-Ca-Sn-Mn alloy, Scripta Materialia, 200 (2021) 113924. https://doi.org/10.1016/j.scriptamat.2021.113924

[5] J. Du, A. Zhang, Z. Guo, M. Yang, M. Li, S. Xiong, Atomic cluster structures, phase stability and physicochemical properties of binary Mg-X (X= Ag, Al, Ba, Ca, Gd, Sn, Y and Zn) alloys from ab-initio calculations, Intermetallics, 95 (2018) 119–129. https://doi.org/10.1016/j.intermet.2018.02.005

[6] C.Y. Ma, C. Wang, Z.M. Hua, P.Y. Wang, J.G. Wang, H.Y. Wang, A high-performance Mg-Al-Sn-Zn-Bi alloy fabricated by combining sub-rapid solidification and hot rolling, Materials Characterization, 169 (2020) 110580. https://doi.org/10.1016/j.matchar.2020.110580

[7] M.Z. Bian, T.T. Sasaki, T. Nakata, Y. Yoshida, N. Kawabe, S. Kamado, K. Hono , Bake-hardenable Mg–Al–Zn–Mn–Ca sheet alloy processed by twin-roll casting, Acta Materialia, 158 (2018) 278–288. https://doi.org/10.1016/j.actamat.2018.07.057

[8] Y. Chai, B. Jiang, J. Somg, Q. Wang, H. Gao, B. Liu, G. Huamg, D. Zhang, F. Pan, Improvement of mechanical properties and reduction of yield asymmetry of extruded Mg-Sn-Zn alloy through Ca addition, Journal of Alloys and Compounds, 782 (2019)1076–1086. https://doi.org/10.1016/j.jallcom.2018.12.109

[9] Q. Wang, B. Jiang, A. Tang, J. Fu, Z. Jiang, H. Sheng, D. Zhang, G. Huang, F. Pan, Unveiling annealing texture formation and static recrystallization kinetics of hot-rolled Mg-Al-Zn-Mn-Ca alloy, Journal of Materials Science & Technology, 43 (2020) 104–118. https://doi.org/10.1016/j.jmst.2020.01.018

[10] Y. Shi, X.Q. Liu, Z.L. Liu, H.J. Xie, H.Y. Wang, J. Li, Effect of Zn content on corrosion behavior of Mg-Y-Zn alloys. Journal of Mining and Metallurgy, Section B: Metallurgy, 58(1) (2022) 51–61. https://doi.org/10.2298/JMMB210525048S

[11] V. Goryany, P. J. Mauk, Intermetallic compounds and choice of alloying elements for the manufacture of thixomolded creepresistant magnesium alloys, Journal of Mining and Metallurgy, Section B: Metallurgy, 43(1) (2007) 85–97. http://doi.org/10.2298/JMMB0701085G

[12] H. Dieringa, Y. Huang, P. Wittke, M. Klein, F. Walther, M. Dikovits, C. Poletti, Compression-creep response of magnesium alloy DieMag422 containing barium compared with the commercial creep-resistant alloys AE42 and MRI230D, Materials Science and Engineering: A, 585 (2013) 430–438. https://doi.org/10.1016/j.msea.2013.07.041

[13] J. Buha, The effect of Ba on the microstructure and age hardening of an Mg-Zn alloy, Materials Science and Engineering: A, 491 (2008) 70–79. https://doi.org/10.1016/j.msea.2008.01.027

[14] Z. Gu, Y. Zhou, Q. Dong, G. He, J. Cui, J. Tan, X. Chen, B. Jiang, F. Pan, J. Eckert, Designing lightweight multicomponent magnesium alloys with exceptional strength and high stiffness, Materials Science and Engineering: A, 855 (2022). https://doi.org/10.1016/j.msea.2022.143901.

[15] P.Y. Wang, B.Y. Wang, C. Wang, J.G. Wang, C.Y. Ma, J.S. Li, M. Zha, H.Y. Wang, Design of multicomponent Mg–Al–Zn–Sn–Bi alloys with refined microstructure and enhanced tensile properties, Materials Science and Engineering: A, 791 (2020) 139696. https://doi.org/10.1016/j.msea.2020.139696

[16] K.S. Tun, A. Kumar, M. Gupta, Introducing a high performance Mg-based multicomponent alloy as an alternative to Al-alloys, Frontiers in Materials, 6 (2019) 1–6. http://doi.org/10.3389/fmats.2019.00215

[17] J. Hu, X. Zhang, C. Tang, Y. Deng, Z. Liu, L. Yang, Microstructures and mechanical properties of the Mg-8Gd-4Y-Nd-Zn-3Si (wt%) alloy, Materials Science and Engineering: A, 571 (2013) 19–24. https://doi.org/10.1016/j.msea.2013.01.056

[18] D. Zhao, X. Chen, Y. Yuan, F. Pan, Development of a novel Mg–Y–Zn–Al–Li alloy with high elastic modulus and damping capacity, Materials Science and Engineering: A, 790 (2020) 139744. https://doi.org/10.1016/j.msea.2020.139744

[19] D. Wang, S. Liu, R. Wu, S. Zhang, Y. Wang, H. Wu, J. Zhang, L. Hou, Synergistically improved damping, elastic modulus and mechanical properties of rolled Mg-8Li-4Y–2Er-2Zn-0.6Zr alloy with twins and long-period stacking ordered phase, Journal of Alloys and Compounds, 881 (2021) 160663. https://doi.org/10.1016/j.jallcom.2021.160663

[20] M. Zubair, Co-deformation between the metallic

matrix and intermetallic phases in a creep-resistant Mg-3.68 Al-3.18 Ca alloy, Materials & Design, 210 (2021) 110113. https://doi.org/10.1016/j.matdes.2021.110113

[21] A.K. Singh, N. Kumar, A. Dwivedi, A. Subramaniam, A geometrical parameter for the formation of disordered solid solutions in multi-component alloys, Intermetallics, 53 (2014) 112–119. https://doi.org/10.1016/j.intermet.2014.04.019

[22] X. Yang, Y. Zhang, Prediction of high-entropy stabilized solid-solution in multi-component alloys, Materials Chemistry and Physics, 132 (2012) 233–238. https://doi.org/10.1016/j.matchemphys.2011.11.021

[23] A. Takeuchi, A. Inoue, Mixing enthalpy of liquid phase calculated by miedema's scheme and approximated with sub-regular solution model for assessing forming ability of amorphous and glassy alloys, Intermetallics, 18(9) (2010) 1779–1789. https://doi.org/10.1016/j.intermet.2010.06.003

[24] P. Maier, D. Ginesta, B. Clausius, N. Hort,. Observations of microstructure-oriented crack growth in a cast Mg-Al-Ba-Ca alloy under tension, compression and fatigue. Metals (Basel), 12 (2022). https://doi.org/10.3390/met12040613

[25] Z.L. Bryan, R.J. Hooper, H.B. Henderson, M.V. Manuel, Solidification pathways of alloys in the Mg-rich corner of the Mg-Al-Ba ternary system, Metallurgical and Materials Transactions A, 46 4 (2015) 1689–1696. https://doi.org/10.1007/s11661-014-2730-2

[26] H.A. Elamami, A. Incesu, K. Korgiopoulos, M. Pekguleryuz, A. Gungor, Phase selection and mechanical properties of permanent-mold cast Mg-Al-Ca-Mn alloys and the role of Ca/Al ratio, Journal of Alloys and Compounds, 764 (2018) 216–225. https://doi.org/10.1016/j.jallcom.2018.05.309.

[27] B. Kondori, R. Mahmudi, Effect of Ca additions on the microstructure, thermal stability and mechanical properties of a cast AM60 magnesium alloy, Materials Science and Engineering: A, 527 (2010) 2014–2021. https://doi.org/10.1016/j.msea.2009.11.043.

[28] L. Zhang, K.K. Deng, K.B. Nie, F.J. Xu, K. Su, W. Liang, Microstructures and mechanical properties of Mg-Al-Ca alloys affected by Ca/Al ratio, Materials Science and Engineering: A, 636 (2015) 279–288. https://doi.org/10.1016/j.msea.2015.03.100

[29] M. Zubair, S. Sandlöbes, M.A. Wollenweber, C.F. Kusche, W. Hildebrandt, S. Korte-Kerzel, On the role of laves phases on the mechanical properties of Mg-Al-Ca alloys, Materials Science and Engineering: A, 756 (2019) 272–283. https://doi.org/10.1016/j.msea.2019.04.048.

[30] F. Wang, T. Hu, Y. Zhang, W. Xiao, C. Ma. Effects of Al and Zn contents on the microstructure and mechanical properties of Mg-Al-Zn-Ca magnesium alloys. Materials Science and Engineering: A, 704 (2017) 57–65. https://doi.org/10.1016/j.msea.2017.07.060

[31] A. Yang, K.B. Nie, K.K. Deng, J.G. Han, T. Xiao, X.Z. Han, Microstructures and tensile properties of Mg-2Zn-0.8Sr-0.2Ca alloy extruded at relatively slow speed and low temperature. Journal of Mining and Metallurgy, Section B: Metallurgy, 58(2) (2022) 203–18. https://doi.org/10.2298/JMMB210325004Y

[32] J. Zhang, Y. Dou, G. Liu, Z. Guo, First-principles study of stacking fault energies in Mg-based binary alloys, Computational Materials Science, 79 (2013) 564–569. https://doi.org/10.1016/j.commatsci.2013.07.012

[33] W. Zhang, Z. Feng, X. Li, Y. Chen, Effect of Zr content on the distribution characteristic of the 14H and 18R LPSO phases, Materials Research, 23(1) (2020) 1–8. https://doi.org/10.1590/1980-5373-MR-2019-0539

[34] Y. Zhang, Y.J. Zhou, J.P. Lin, G.L. Chen, P.K. Liaw, Solid-solution phase formation rules for multi-component alloys, Advanced Engineering Materials, 10(6) (2008) 534–538. https://doi.org/10.1002/adem.200700240

[35] A.R. Miedema, P.F. de Châtel, F.R. de Boer, Cohesion in alloys - fundamentals of a semi-empirical model, Physica B+C, 100(1) (1980) 1–28. https://doi.org/10.1016/0378-4363(80)90054-6

[36] S. Guo, C. Ng, J. Lu, C.T. Liu, Effect of valence electron concentration on stability of fcc or bcc phase in high entropy alloys, Journal of Applied Physics, 109(10) (2011) 103505. https://doi.org/10.1063/1.3587228

[37] A. Takeuchi, A. Inoue, Quantitative evaluation of critical cooling rate for metallic glasses, Materials Science and Engineering: A, 304–306(1–2) (2001) 446–451. https://doi.org/10.1016/S0921-5093(00)01446-5

[38] D. B. Miracle, O. N. Senkov, A critical review of high entropy alloys and related concepts, Acta Materialia, 122 (2017) 448–511. https://doi.org/10.1016/j.actamat.2016.08.081.

[39] A. Kumar, M. Gupta, An insight into evolution of light weight high entropy alloys: A review, Metals (Basel), 6(9) (2016) 199. https://doi.org/10.3390/met6090199.

[40] M. Sadeghi, B. Niroumand, Design and characterization of a novel MgAlZnCuMn low melting point light weight high entropy alloy (LMLW-HEA), Intermetallics, 151 (2022) 107658. https://doi.org/10.1016/j.intermet.2022.107658

[41] J.W. Yeh, Alloy design strategies and future trends in high-entropy alloys, The Journal of The Minerals, Metals & Materials Society, 65 12 (2013) 1759–1771 https://doi.org/10.1007/s11837-013-0761-6

[42] H.Z. Qu, F.F. Liu, B.Y. Gao, J. Bai, Q.Z. Gao, S. Li, Microstructure, mechanical properties and magnetic properties of FeCoNiCuTiSix high-entropy alloys, Science China Technological Sciences, 63(3) (2020) 459–466. https://doi.org/10.1007/s11431-019-9549-9

[43] Y. Zhang, D. Wang, S. Wang, High-entropy alloys for electrocatalysis: Design, characterization, and applications, Small, 18(7) (2022). https://doi.org/10.1002/smll.202104339

[44] J. Rong, W. Xiao, Y. Fu, X. Zhao, P. Yan, C. Ma, M. Chen, C. Huang, A high performance Mg–Al–Ca alloy processed by high pressure die casting: Microstructure, mechanical properties and thermal conductivity, Materials Science and Engineering: A, 849 (2022). https://doi.org/10.1016/j.msea.2022.143500

[45] S.W. Xu, N. Matsumoto, K. Yamamoto, S. Kamado, T. Honma, Y. Kojima, High temperature tensile properties of as-cast Mg-Al-Ca alloys, Materials Science and Engineering: A, 509 (1–2) (2009) 105–110. https://doi.org/10.1016/j.msea.2009.02.024

[46] L. Han, H. Hu, D.O. Northwood, N. Li, Microstructure and nano-scale mechanical behavior of Mg-Al and Mg-Al-Ca alloys, Materials Science and Engineering: A, 473(1–2) (2008) 16–27.

https://doi.org/10.1016/j.msea.2007.03.053

[47] M. Zubair, S. Sandlöbes-Haut, M.A. Wollenweber, K. Bugelnig, C.F. Kusche, G. Requena, Strain heterogeneity and micro-damage nucleation under tensile stresses in an Mg–5Al–3Ca alloy with an intermetallic skeleton, Materials Science and Engineering: A, 767 (2019) 138414. https://doi.org/10.1016/j.msea.2019.138414

[48] S. Luo, L. Wang, J. Wang, G. Zhu, X. Zeng, Micro-compression of Al2Ca particles in a Mg-Al-Ca alloy, Materialia, 21 (2022). https://doi.org/10.1016/j.mtla.2021.101300

[49] S. Abaspour, C.H. Cáceres, Thermodynamics-based selection and design of creep-resistant cast Mg alloys, Metallurgical and Materials Transactions A, 46(12) (2015) 5972–5988. https://doi.org/10.1007/s11661-015-3128-5

[50] J. Bočan, J. Maňák, A. Jäger, Nanomechanical analysis of AZ31 magnesium alloy and pure magnesium correlated with crystallographic orientation, Materials Science and Engineering: A, 644 (2015) 121–128. https://doi.org/10.1016/j.msea.2015.07.055.

ISPITIVANJE MIKROSTRUKTURNIH, MEHANIČKIH I TERMODINAMIČKIH SVOJSTAVA NOVE MULTIKOMPONENTNE LEGURE Mg-15Al-8Ca-3Zn-2Ba BEZ ELEMENATA RETKE ZEMLJE

Y. Türe

Tehnički univerzitet Eskisehir, Stručna škola Porsuk, Odsek za elektroniku i automatizaciju, Program mehatronike, Eskisehir, Turska

Apstrakt

Napori u istraživanju i razvoju značajno se povećavaju kako bi se zadovoljila rastuća potražnja za ekološki prihvatljivim legurama magnezijuma (Mg). Studije trenutno istražuju različite kombinacije legirajućih elemenata kako bi se ispunile zahtevne specifikacije. Cilj ovog rada bio je da se ispita upotrebljivost elemenata aluminijuma (Al), kalcijuma (Ca) i cinka (Zn) zajedno sa barijumom (Ba) i da se ispitaju mehanička i termodinamička svojstva dobijenog sistema višekomponentnih legura. SEM i testovi tvrdoće su korišćeni za ispitivanje mikrostrukturnih i mehaničkih svojstava legura Mg. U SEM analizi se legura sastojala od α-Mg matrice, kompaktne strukture nalik bloku sa Ba ($Mg_{17}Ba_2$), regionalne eutektičke strukture ($Ca_2Mg_6Zn_3$) i nezavisno rastuće lamele (Al_2Ca). Rezultati opšte analize tvrdoće legure, mereni Brinelovim i Vikersovim testovima, utvrđeni su kao ~77 i ~82, pojedinačno. Test udubljenja je takođe pokazao da je prenos napona na Al_2Ca lamelarnu fazu moguć, u zavisnosti od orijentacije ravni klizanja između matrice i Al_2Ca faze. Takođe je uočeno da su se pukotine koje su se razvile na intermetalnoj $Mg_{17}Ba_2$ fazi u testu udubljenja formirale samo u oblastima koje su pod visokim naprezanjem strukture i da je njihovo širenje ograničeno. Prema termodinamičkoj analizi, vrednost je ΔH_{mix} = -2,73 kJ/mol, vrednost ΔS_{mix} je 5,95 J/molK, vrednost δ je 34%, vrednost Δχ je 0,14 i vrednost Ω je 2,03. Utvrđeno je da su dobijeni termodinamički podaci u skladu sa mikrostrukturnom evolucijom legure.

Ključne reči: *Višekomponentna legura Mg; Laka legura; Legura niske entropije (LEA); Mikrostruktura*